Design and preparation of a bulk magnet exhibiting an inverted hysteresis loop

Shin-ichi Ohkoshi, Toshiya Hozumi, and Kazuhito Hashimoto*
Research Center for Advanced Science and Technology, The University of Tokyo, 4-6-1 Komaba, Meguro-ku, Tokyo 153-8904, Japan
(Received 13 March 2001; published 29 August 2001)

We report on a magnet exhibiting an *inverted magnetic hysteresis loop*, i.e., the magnetization becomes negative in the decreasing part even when the applied field is still positive, while the magnetization becomes positive in the increasing part when the applied field is still negative. The key to obtaining this unusual magnet is to utilize a competing effect between the spin-flip transition and the uniaxial magnetic anisotropy. On the basis of the model calculations considering this effect, we have succeeded in synthesizing a bulk magnet showing the inverted magnetic hysteresis loop with the system of samarium(III) gadolinium(III) hexacyanochromate(III).

DOI: 10.1103/PhysRevB.64.132404 PACS number(s): 75.30.Et, 75.50.Gg

Magnetic materials play an important role in modern technology, and various magnets having novel properties are being developed. However, the rational design of new magnets is, in general, difficult with conventional metal alloys and metal oxide magnets. One of the reasons is that, in metal alloys and metal oxides, the substitutions of metals often induce structural distortion. In addition, magnetic moments interact not only between the nearest neighbors but also among second and further nearest neighbors through exchange or superexchange pathways. Therefore, even though theoretical explanations for the magnetic properties of existing magnets are possible, theoretical designs of novel magnets have not been very successful. In contrast, it is believed that molecule-based magnets[1–3] have advantages for the design of magnetic properties. Particularly, the rational design of magnets based on the molecular field theory is effective for the class of cyanide-bridged multimetal complexes, $A1A2[B(CN)_6]\cdot zH_2O$ ($A1$, $A2$, and B are metal ions having unpaired electrons),[4–6] based on the following reasons: (1) metal substitutions induce only small lattice constant changes, and (2) superexchange interactions are essentially effective only between the nearest-neighbor metal ions.[4–9] For example, we have recently succeeded in designing and preparing a type of magnet exhibiting two compensation temperatures with the system of $(Ni^{II}_aMn^{II}_bFe^{II}_c)_{1.5}[Cr^{III}(CN)_6]\cdot 7.5H_2O$ $(a+b+c=1)$, i.e., the spontaneous magnetization changes its sign twice with changing temperature.[6] Moreover, it is relatively easy to add novel functionalities to molecule-based magnets, because magnets can be fabricated by the selection of proper transition metal ions and coordinating ligands. In fact, various functionalized magnets showing photoinduced magnetization,[10] photoinduced magnetic pole inversion,[11] etc., have been reported.

The objective of the present study is to design a magnet exhibiting an anomalous magnetic hysteresis loop. Usually, magnets possess positive values of a remanent magnetization and a coercive field. Recently, however, a negative remanent magnetization was observed in specific exchange-coupled multilayers such as Co/Pt/Gd/Pt and in epitaxial Fe films on W(001).[12–17] These hysteresis loops are called inverted magnetic hysteresis loops. In these materials, their thin film forms play an important role in the origin of the unusual hysteresis loops,[18] and hence, one has considered that these phenomena are limited to *thin-film*-type of magnetic materials. In the present study, however, we try to obtain a *bulk* magnet showing such an *inverted magnetic hysteresis loop*.

The key to designing this unusual magnet is to utilize a competing effect between a spin-flip transition and a uniaxial magnetic anisotropy. Here, let us consider the following magnet composed of three metal ions, $A1$, $A2$, and B, where the A (either $A1$ or $A2$) and B ions are alternately connected and the magnetic couplings between the A and B ions are antiferromagnetic as shown in Fig. 1(a) (their sublattice magnetizations are denoted as M_{A1}, M_{A2}, and M_B, respectively). There is a possibility to observe the inverted hysteresis loop in this ferrimagnet if the following conditions are satisfied, i.e., (1) $|M_{A1}+M_{A2}|$ is close to $|M_B|$, (2) $|M_{A1}|$ is larger than $|M_{A2}|$, and (3) only the $A2$ ion has a large uniaxial magnetic anisotropy (K_u). In the initial magnetization process of this ferrimagnet, the field-induced spin-flip transition is caused by a relatively weak external field (H) due to its small spontaneous magnetization ($M_{\text{total}}=|M_{A1}+M_{A2}|-|M_B|$), where M_B may rotate toward the positive direction of $(+H)$ and M_{A2} toward the opposite direction $(-H)$ due to the antiferromagnetic interaction between M_B and M_{A2} [Fig. 1(b)]. Conversely, in the decreasing part of the hysteresis loop, M_{A1} could rotate toward the $-H$ direction before the rotation of M_B and M_{A2} because of the large K_u of the $A2$ metal ion and the magnetic coupling between M_B and M_{A2} [Fig. 1(c)]. As a result, the remanent magnetization could become a negative value.

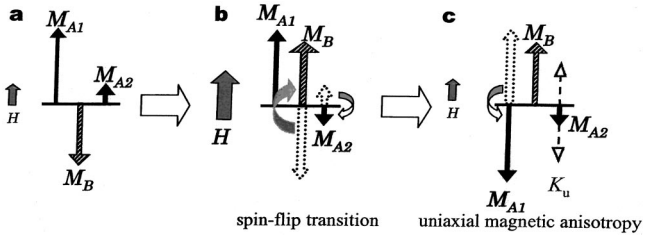

FIG. 1. Schematic illustration of the mechanism of the inverted hysteresis loop for a bulk magnet. M_{A1}, M_{A2}, and M_B represent the sublattice magnetizations of the $A1$, $A2$, and B ions, respectively.

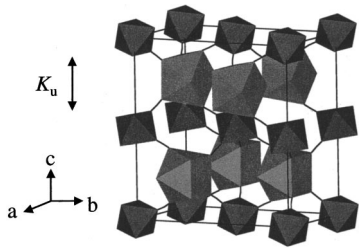

FIG. 2. Schematic structure of orthorhombic $Sm^{III}_{x}Gd^{III}_{1-x}[Cr^{III}(CN)_6]\cdot 4H_2O$ by analogy with the crystal structure of $Sm^{III}[Fe^{III}(CN)_6]\cdot 4H_2O$ [20]. The large and small polyhedrons describe $[Sm^{III}$ (or $Gd^{III})N_6O_2]$ and $[Cr^{III}C_6]$, respectively. Zeolitic water molecules in the unit cell are omitted for clarity. The easy axis of the uniaxial magnetic anisotropy (K_u) is along the c axis of the crystal.

Let us consider a system to meet the requirements mentioned above. The spin-flip transition can be controlled by the magnetization value and the magnitude of the molecular field coefficients. As for the large magnetic anisotropy, rare-earth metal ions are good candidates due to their orbital angular momenta (L). From these points of view, we will consider cyanide-bridged rare-earth metal compounds, $Sm^{III}_{x}Gd^{III}_{1-x}[Cr^{III}(CN)_6]\cdot 4H_2O$ (Sm^{III}, $L=5$, $S=5/2$, $J=L\text{-}S=5/2$, Gd^{III}, $J=S=7/2$, Cr^{III}, $J=S=3/2$), to exemplify our idea (Fig. 2).

We theoretically calculated the magnetic hysteresis loops of this system by considering both the molecular field (n_{ij}) and the uniaxial magnetic anisotropy (K_u). For the $Sm^{III}_{x}Gd^{III}_{1-x}[Cr^{III}(CN)_6]\cdot 4H_2O$ system, only the two types of superexchange couplings between the nearest-neighbor spin sources, Sm-Cr and Gd-Cr, are present and the Sm^{III} ion dominates the uniaxial magnetic anisotropy. The total energy of such a system at zero temperature is then expressed as

$$E = -M_{\mathrm{Sm}}H\cos\theta_{\mathrm{Sm}} - M_{\mathrm{Gd}}H\cos\theta_{\mathrm{Gd}} - M_{\mathrm{Cr}}H\cos\theta_{\mathrm{Cr}} - n_{\mathrm{SmCr}}M_{\mathrm{Sm}}M_{\mathrm{Cr}}\cos(\theta_{\mathrm{Sm}}-\theta_{\mathrm{Cr}}) - n_{\mathrm{GdCr}}M_{\mathrm{Gd}}M_{\mathrm{Cr}} \times\cos(\theta_{\mathrm{Gd}}-\theta_{\mathrm{Cr}}) + xK_u\sin^2(\theta_{\mathrm{Sm}}-\theta_p). \quad (1)$$

The first three terms represent the magnetostatic energies of the sublattice magnetizations, where θ_{Sm}, θ_{Gd}, and θ_{Cr} are the angles of the directions M_{Sm}, M_{Gd}, and M_{Cr} from the H direction, respectively. The next two terms are the molecular fields between the nearest-neighbor sites, where n_{SmCr} and n_{GdCr} are the molecular field coefficients of Sm-Cr and Gd-Cr, respectively. The last term describes the uniaxial magnetic anisotropy due to the Sm^{3+} ion with K_u. From the observed T_N values for $x=0$ and 1, the n_{GdCr} and n_{SmCr} were estimated to be -3.2 and -30.4, respectively. In addition, the K_u value in the Sm^{3+}-substituted iron garnet was reported to be 1.3×10^6 J/m^3 at 4.2 K.[19] Using these values, the numerical calculation of the magnetic hysteresis loop was carried out.

The calculated results showed that the inverted hysteresis loops are obtained for the compounds with x around 0.5. As the best example of the calculations, we show the calculated results for $x=0.52$. Figure 3(a) shows the hysteresis loops at

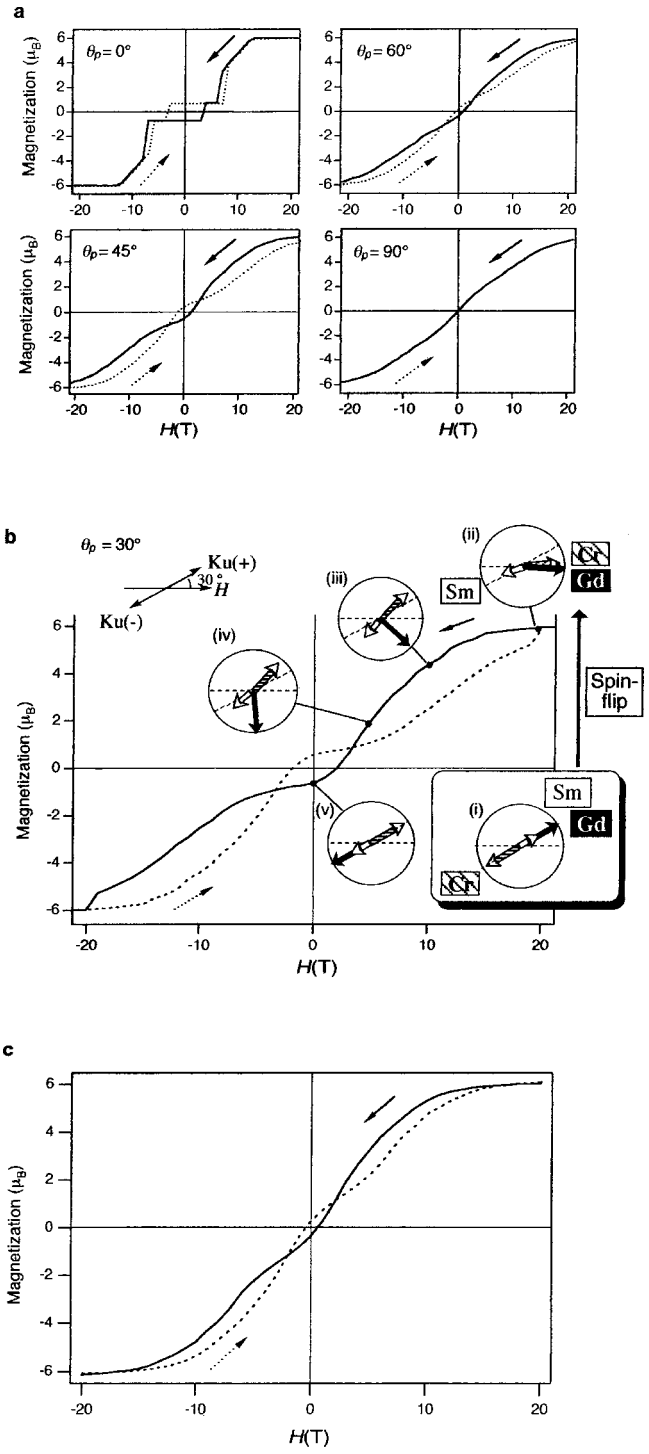

FIG. 3. (a) The numerical calculation of magnetic hysteresis loops for $Sm^{III}_{0.52}Gd^{III}_{0.48}[Cr^{III}(CN)_6]\cdot 4H_2O$ at θ_p values of 0°, 45°, 60°, and 90°. The solid and dotted lines describe the decreasing and increasing parts of the magnetic hysteresis loops, respectively. (b) The magnetization configuration of the sublattice magnetizations for $\theta_p=30°$ as a function of H. The arrows in the circles of (i)–(v) show the directions of the sublattice magnetizations, M_{Gd} (black arrow), M_{Sm} (white arrow), and M_{Cr} (shadow arrow), respectively, from the H direction. (c) The calculated magnetic hysteresis loop for the powder sample for $Sm^{III}_{0.52}Gd^{III}_{0.48}[Cr^{III}(CN)_6]\cdot 4H_2O$, considering the distribution of crystalline orientation.

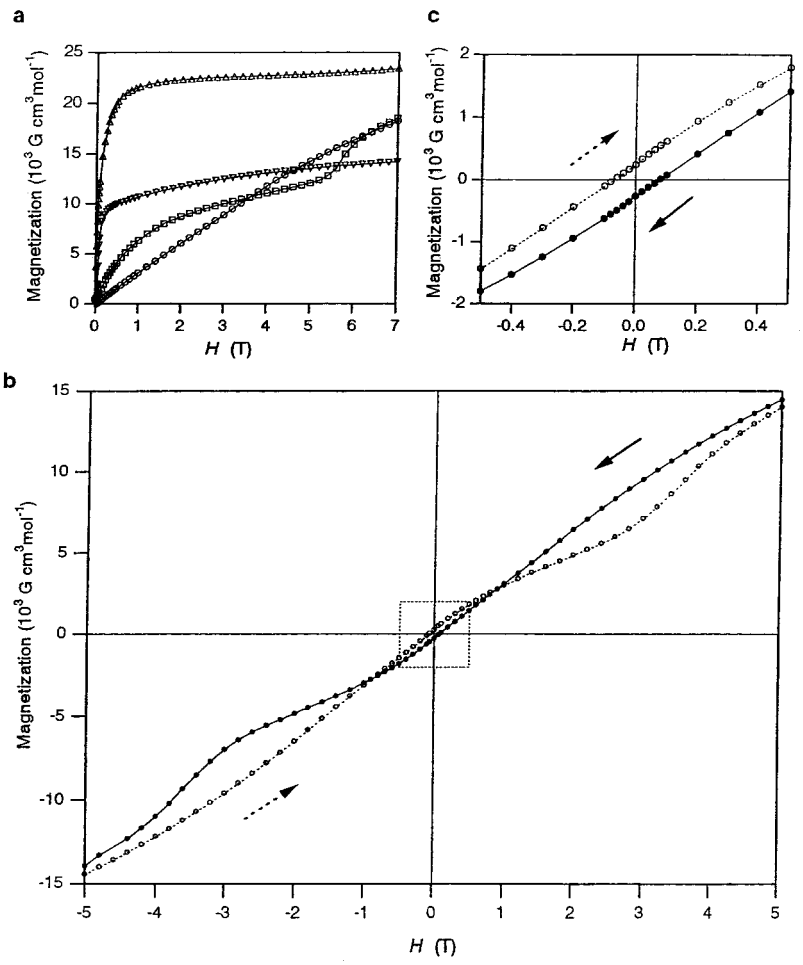

FIG. 4. (a) Magnetization processes with increasing H for the compounds $Sm^{III}_x Gd^{III}_{1-x}[Cr^{III}(CN)_6]\cdot 4H_2O$; $x=0$ ($\triangle$), 0.36 ($\square$), 0.52 ($\bigcirc$), and 1 ($\triangledown$), at 2 K. (b) The magnetic hysteresis loops for $x=0.52$ in the applied magnetic field between $+7$ and -7 T at 2 K. The solid and dotted lines describe the decreasing and increasing parts of the magnetic hysteresis loops, respectively. (c) Enlarged plots of the dotted square in the magnetic hysteresis loop of (b).

various angles (θ_p) of the magnetic easy axis from the H direction, showing the inverted hysteresis loop in the wide range of $0°\leqslant\theta_p\leqslant 70°$. In Fig. 3(b) are shown the configurations of the sublattice magnetizations for $\theta_p=30°$ for different H values together with its hysteresis loop. Initially, M_{Sm} and M_{Gd} are positive magnetizations and M_{Cr} is a negative one at low H because $|M_{Sm}+M_{Gd}|$ of nitrogen ends is larger than $|M_{Cr}|$ of carbon ends for this composition [(i) in Fig. 3(b)]. However, when the spin-flip transition takes place at high H, M_{Gd} and M_{Cr} are oriented parallel to the $+H$ direction and M_{Sm} is oriented to the $K_u(-)$ direction [(ii) in Fig. 3(b)]. With decreasing H, i.e., in the decreasing part of the hysteresis loop, M_{Gd} rotates toward the $-H$ direction [(iii), (iv) in Fig. 3(b)]. When H becomes close to zero, M_{Sm} and M_{Gd} are then oriented to the $K_u(-)$ direction and M_{Cr} is oriented to the $K_u(+)$ direction [(v) in Fig. 3(b)]. The signs of these sublattice magnetizations ($M_{Sm}<0, M_{Gd}<0, M_{Cr}>0$) in (v) are opposite to those of the initial sublattice magnetizations ($M_{Sm}>0, M_{Gd}>0, M_{Cr}<0$) in (i). As a result, the directions of the resulting sublattice magnetizations are opposite to those of the initial sublattice magnetizations. These calculations in Figs. 3(a) and 3(b) correspond to the hysteresis loops for a single-crystalline sample with different angles of the magnetic easy axis from the H direction. For the samples in powder form, we have to consider the anisotropic distribution of the crystalline orientation. The result is shown in Fig. 3(c). The powder pattern calculation also shows the *inverted hysteresis loop*.

On the basis of the above calculations, we have prepared the powder samples of $Sm^{III}_x Gd^{III}_{1-x}[Cr^{III}(CN)_6]\cdot 4H_2O$ by the procedures described in Ref. 20. The X-ray powder diffraction (XRD) patterns showed that the prepared materials have an orthorhombic structure (*Cmcm*) as shown in Fig. 2. Their lattice constants continuously changed as a function of x; $a=7.541$, $b=13.096$, and $c=14.046$ Å ($x=0$) to $a=7.596$, $b=13.110$, and $c=14.099$ Å ($x=1$). The CN stretching frequencies in the IR spectra also continuously changed depending on x; 2163 and 2155 cm^{-1} ($x=0$) to 2160 and 2152 cm^{-1} ($x=1$). These successive shifts of the XRD and IR peaks indicate that the Sm^{III} and Gd^{III} ions are randomly coordinated to the nitrogen ends of the cyano groups. By analogy with the crystal structure of $Sm^{III}[Fe^{III}(CN)_6]\cdot 4H_2O$,[21] it is suggested that the Sm^{III} and Gd^{III} ions are bound to six cyanonitrogen atoms and two water molecules in a square antiprism geometry (D_{4d}), and the Cr^{III} ion is octahedrally bound to the cyanocarbon (O_h).

Magnetization measurements for the prepared $Sm^{III}_x Gd^{III}_{1-x}[Cr^{III}(CN)_6]\cdot 4H_2O$ powders were carried out using a superconducting quantum interference device magnetometer. Polycrystalline samples (~20 mg) were loaded into gelatin capsules. The magnetization versus temperature curves showed that elemental $Gd^{III}[Cr^{III}(CN)_6]\cdot 4H_2O$($x$

$=0$) and $Sm^{III}[Cr^{III}(CN)_6]\cdot 4H_2O(x=1)$ were ferrimagnets with Néel temperature (T_N) values of 10.2 and 10.5 K, respectively, which are consistent with the literature values.[22] The T_N values for the compounds with the intermediate x were maintained between these two T_N values. The M_s values systematically changed depending on x. For the compounds with x between zero and 0.53, the M_s values linearly decreased from $3.9\mu_B$ to zero with increasing x. In contrast, in the range of $0.53<x\leqslant 1$, the M_s values linearly increased from zero to $2.0\mu_B$ with increasing x. These results can be explained by a similar mechanism for $(Ni^{II}_xMn^{II}_{1-x})_{1.5}[Cr^{III}(CN)_6]\cdot 7.5H_2O$,[4] i.e., the M_s values are determined by the sum of the sublattice magnetizations of $Gd^{III}(M_{Gd})$ and $Sm^{III}(M_{Sm})$ and antiparallel sublattice magnetization of $Cr^{III}(M_{Cr})$. The magnetization versus H curves showed the upturn changes in the magnetization, e.g., 6.0 T ($x=0.27$), 5.4 T ($x=0.36$), 3.8 T ($x=0.44$), and 0 T ($x=0.52$), as shown in Fig. 4(a). Particularly, for the materials around $x=0.52$, the upturn changes took place at $H\approx 0$. The observed upturn changes in the magnetization are caused by the spin-flip transition due to the small magnetization value. The magnetic hysteresis loops were measured in the region of $-7\leqslant H\leqslant 7$ T at 2 K. The compounds with $0\leqslant x\leqslant 0.50$ and $0.53\leqslant x\leqslant 1$ showed the normal magnetic hysteresis loops. In the hysteresis loops for $x=0.51$ and 0.52, however, the magnetization became negative in the decreasing part when the applied field was still positive, while the magnetization became positive in the increasing part when the applied field was still negative. The inverted magnetic hysteresis loops were thus observed in these compositions. Figures 4(b) and 4(c) show the inverted magnetic hysteresis loop for $x=0.52$ at 2 K. The remanent magnetization and coercive field were *negative* values of -260 G cm^3 mol^{-1} and -800 G, respectively. This experimental hysteresis loop qualitatively corresponds to the calculated hysteresis loop, indicating that the observation of the inverted hysteresis loop can be reasonably explained by the competition between the sublattice magnetization rotation due to the spin-flip transition and the trapping effect due to the uniaxial magnetic anisotropy, based on our scenario.

We have thus succeeded in obtaining a novel magnet having inverted magnetic hysteresis loops by controlling the various magnetic parameters such as the magnetization values, molecular fields, and the uniaxial magnetic anisotropy. It should be emphasized that the present mechanism is essentially different from the mechanisms of the inverted hysteresis loops in specific exchange-coupled multilayer films or epitaxial Fe films. The existence of such a bulk magnet allows us to postulate many ideas, e.g., how does the magnetic domain pattern change depending on the external magnetic field? Moreover, our strategy could be applied to high-T_c magnets composed of metal alloys and metal oxides. The theoretical and experimental studies along this line are now under way.

*Author to whom correspondence should be addressed.

[1] J. S. Miller and A. J. Epstein, Angew. Chem. Int. Ed. Engl. **33**, 385 (1994).
[2] O. Kahn, *Molecular Magnetism* (VCH, New York, 1993).
[3] P. Day and A. E. Underhill, Philos. Trans. R. Soc. London, Ser. A **357**, 2849 (1999).
[4] S. Ohkoshi, T. Iyoda, A. Fujishima, and K. Hashimoto, Phys. Rev. B **56**, 11 642 (1997).
[5] S. Ohkoshi and K. Hashimoto, Phys. Rev. B **60**, 12 820 (1999).
[6] S. Ohkoshi, Y. Abe, A. Fujishima, and K. Hashimoto, Phys. Rev. Lett. **82**, 1285 (1999).
[7] S. Ferlay, T. Mallah, R. Ouahés, P. Veillet, and M. Verdaguer, Nature (London) **378**, 701 (1995).
[8] S. M. Holmes and G. S. Girolami, J. Am. Chem. Soc. **121**, 5593 (1999).
[9] Ø. Hatlevik, W. E. Bushmann, J. Zhang, J. L. Manson, and J. S. Miller, Adv. Mater. **11**, 914 (1999).
[10] O. Sato, T. Iyoda, A. Fujishima, and K. Hashimoto, Science **272**, 704 (1996).
[11] S. Ohkoshi and K. Hashimoto, J. Am. Chem. Soc. **121**, 10 591 (1999).
[12] C. A. Chang, Appl. Phys. Lett. **57**, 297 (1990).
[13] N. K. Flevaris and R. Krishnan, J. Magn. Magn. Mater. **104–107**, 1760 (1992).
[14] K. Takanashi, H. Kurokawa, and H. Fujimori, Appl. Phys. Lett. **63**, 1585 (1993).
[15] C. Gao and M. J. O'Shea, J. Magn. Magn. Mater. **127**, 181 (1993).
[16] J. Chen and J. L. Erskine, Phys. Rev. Lett. **68**, 1212 (1992).
[17] M. C. dos Santos, J. Geshev, J. E. Schmidt, S. R. Teixeira, and L. G. Pereira, Phys. Rev. B **61**, 1311 (2000).
[18] The inverted hysteresis loops in the exchange-coupled multilayers such as the Co/Pt/Gd/Pt/films are explained by a combination between the antiferromagnetic coupling among the layers and the magnetic anisotropy acting on only the side layer (Refs. 12–15). Conversely, those in the heteroepitaxial Fe films on W(001) or Si(111) originate from the competition between the cubic and uniaxial magnetic anisotropy in the isolated Fe microcrystallines (Refs. 16 and 17).
[19] P. Hansen, in *Physics of Magnetic Garnets*, Proceedings of the International School of Physics ''Enrico Fermi,'' Course LXX, Varenna, 1978, edited by A. Paoletti (Academic, London, 1978), p. 56.
[20] The $Sm^{III}_xGd^{III}_{1-x}[Cr^{III}(CN)_6]\cdot 4H_2O$ powders were prepared by reacting an aqueous solution containing mixtures of $SmCl_3$ and $GdCl_3$ with a $K_3Cr(CN)_6$ aqueous solution at 55 °C to yield a light yellow precipitate. Elemental analyses for Sm, Gd, and Cr were obtained by inductively coupled plasma mass spectrometry, e.g., Calculated for $Sm_{0.27}Gd_{0.73}[Cr(CN)_6]\cdot 4H_2O$:Sm, 9.3; Gd, 26.4; Cr, 11.9, and found: Sm, 9.4; Gd, 26.7; Cr, 12.1 Calculated for $Sm_{0.52}Gd_{0.48}[Cr(CN)6]\cdot 4H_2O$:Sm, 18.2; Gd, 17.2; Cr, 12.0, and found: Sm, 18.7; Gd, 17.5; Cr, 12.8. Calculated for. $Sm_{0.60}Gd_{0.40}[Cr(CN)_6]\cdot 4H_2O$:Sm, 20.5; Gd, 14.9; Cr, 12.0, and found: Sm, 20.8; Gd, 14.5; Cr, 12.1.
[21] W. Petter, V. Gramlich, and F. Hulliger, J. Solid State Chem. **82**, 161 (1989).
[22] F. Hulliger, M. Landolt, and H. Vetsch, J. Solid State Chem. **18**, 283 (1976).